Annu. Rev. Biomed. Eng. 2004. 6:249–73
doi: 10.1146/annurev.bioeng.6.040803.140055
Copyright © 2004 by Annual Reviews. All rights reserved
First published online as a Review in Advance on February 6, 2004

OCULAR BIOMECHANICS AND BIOTRANSPORT

C. Ross Ethier,[1] Mark Johnson,[2] and Jeff Ruberti[3]
[1]*Departments of Mechanical and Industrial Engineering, Ophthalmology, and Institute for Biomaterials and Biomedical Engineering, University of Toronto, Ontario, M5S 3G8, Canada; email: ethier@mie.utoronto.ca*
[2]*Department of Biomedical Engineering, Northwestern University, Evanston, Illinois 60208; email: m-johnson2@northwestern.edu*
[3]*Cambridge Polymer Group, Inc., Somerville, Massachusetts 02143, and Adjunct Assistant Scientist, Schepens Eye Research Institute, Boston, Massachusetts 02114-2500; email: jeff@campoly.com*

Key Words cornea, glaucoma, aqueous humor drainage, optic nerve head, Bruch's membrane

■ **Abstract** The eye transduces light, and we usually do not think of it as a biomechanical structure. Yet it is actually a pressurized, thick-walled shell that has an internal and external musculature, a remarkably complex internal vascular system, dedicated fluid production and drainage tissues, and a variety of specialized fluid and solute transport systems. Biomechanics is particularly involved in accommodation (focusing near and far), as well as in common disorders such as glaucoma, macular degeneration, myopia, and presbyopia. In this review, we give a (necessarily brief) overview of many of the interesting biomechanical aspects of the eye, concluding with a list of open problems.

CONTENTS

INTRODUCTION 250
Overview of Ocular Anatomy 250
OCULAR BIOSOLID MECHANICS 250
Mechanics of the Sclera and Corneoscleral Envelope 251
Corneal Biomechanics 253
Retina and Lamina Cribrosa Biomechanics 256
Accommodation and Presbyopia 257
OCULAR BIOFLUID MECHANICS AND TRANSPORT 257
Blood Flow in the Eye 258
Aqueous Humor Dynamics 259
Transport Within the Cornea 261
Transport Across Bruch's Membrane 263
Scleral Permeability and Drug Delivery to the Eye 263
SUMMARY AND OPEN PROBLEMS 266

INTRODUCTION

The eye is a remarkable organ, specialized for the conversion of photons into spatially organized and temporally resolved electrochemical signals. Biomechanics plays a major role in the normal and pathological function of the eye. We begin with a brief anatomical review of some of the biomechanically important parts of the eye.

Overview of Ocular Anatomy

The outer envelope of the eye is formed by two connective tissues, the cornea and sclera (Figure 1). Six extraocular muscles attach to the outer sclera, acting to rotate the eye in concert with a clever system of active pulleys (1). The corneoscleral envelope forms a closed shell, pierced at the back of the eye by the scleral canal and at other discrete locations by small vessels and nerves. The optic nerve, responsible for carrying information from the retina to the visual center in the brain, leaves the eye through the scleral canal. Light enters the eye by passing through the cornea, after which it traverses the anterior chamber, pupil, lens, and vitreous body before striking the retina. The lens is suspended by ligaments (the zonules) that attach to the inner fibers of the ciliary muscle; alterations in tone of these muscle fibers cause the zonules to tug on the lens, so that the lens changes shape to alter the focal length of the eye in a process known as accommodation.

The ciliary body consists of the ciliary muscle and a highly folded and vascularized inner layer known as the ciliary processes, which secrete a clear, colourless fluid called the aqueous humor. This fluid flows radially inward, bathing the lens, then flows anteriorly through the pupil to fill the anterior chamber and nourish the cornea, before draining out of the eye through specialized tissues in the angle formed by the iris and cornea. As we will see, this fluid flow is responsible for creating a positive pressure within the eye, the so-called intraocular pressure (IOP), which has many interesting biomechanical consequences. Additionally, the volume of vascular beds within the eye changes throughout the cardiac cycle, creating a time-varying component of the IOP in an effect known as the ocular pulse. The space behind the lens is filled with a relatively inert connective tissue called the vitreous body. It is quite porous and thus transmits the pressure from the anterior chamber throughout the interior of the eye.

OCULAR BIOSOLID MECHANICS

The eye is subjected to a mean and time-varying internal pressure; furthermore, the ciliary muscle can create significant internal forces, whereas the extraocular muscles create external forces. Despite these forces, the eye must maintain the proper relative positions of all optical components so as to ensure high visual acuity. This leads to some interesting biosolid mechanics.

Mechanics of the Sclera and Corneoscleral Envelope

The corneoscleral shell encloses the intraocular tissues and protects the eye from blunt injury. It is a surprisingly tough tissue that has a high elastic modulus and a very high rupture strength. Measurements on intact inflated human ocular globes have yielded average Young's moduli in the range of 5–13 MPa (3–5). The sclera is largely composed of circumferentially oriented types I and III collagen fibers and thus has a modulus in the circumferential direction much higher than in the radial (6).

Knowledge of the elastic properties of the sclera is important in several applications: improving the accuracy of methods to measure IOP and resistance to aqueous humor drainage, understanding the development of myopia (near-sightedness), and interpreting the magnitude of the ocular pulse. We first review the many studies done to measure mechanical properties of the sclera and to model the stress-strain behavior of the corneoscleral envelope. Then we examine the application of these findings.

Friedenwald (7) first proposed the "ocular rigidity function," describing the change in intraocular pressure, (IOP–IOP_0), with a change in ocular volume, ($V - V_0$):

$$\ln\left[\frac{IOP}{IOP_0}\right] = K(V - V_0), \tag{1}$$

where K is the coefficient of ocular rigidity. In humans, K is approximately 0.05 μl^{-1} (8), giving a compliance of the ocular envelope of roughly 1 μl/mmHg at a physiologic IOP of 15 mmHg; the bovine eye is considerably less stiff with an ocular rigidity that is roughly tenfold smaller.

Equation 1 is consistent with the mechanical properties of collagen, which is responsible for the high elastic modulus of the sclera. Specifically, collagen exhibits a stress (σ)/strain (ε) relationship of the form (9)

$$\sigma = A[e^{\alpha\varepsilon} - 1], \tag{2}$$

where A and α are material constants. Note that at low strains, Aα is equivalent to the Young's modulus of the material.

The tangential (hoop) stress in the sclera can be related to the intraocular pressure using Laplace's relation: $\sigma = IOP\, R/(2h)$, where R is the radius of the eye and h is the thickness of the sclera. Considering small strains, such that $\varepsilon = (R - R_0)/R_0$ (but not so small that Equation 2 is linear), we let $V - V_0 = 4\pi\, R_0^2\, (R - R_0)$. Approximating Equation 2 as $\sigma = A \exp(\alpha\, \varepsilon)$, Equation 1 results. The approximation is reasonable when strains are large enough that the nonlinear term dominates Equation 2, which occurs for very small strains indeed because α is very large. Keeping the full form of Equation 2 leads to a modified form of the

Friedenwald equation (in the small strain limit):

$$\ln\left[\frac{IOP + \dfrac{2hA}{R}}{IOP_0 + \dfrac{2hA}{R}}\right] = \frac{\alpha}{V_0}(V - V_0). \tag{3}$$

McEwen & St. Helen (10) first introduced Equation 3, and Collins & Van der Werff (8) summarized their results for human eyes to obtain $\alpha/V_0 = 0.022\ \mu l^{-1}$ and $2hA/R = 9.5$ mmHg. If we let the typical radius and thickness of the human corneoscleral shell be 1.15 cm and 0.06 cm, respectively (8), then $\alpha = 140$ and the low strain modulus, $A\alpha$, is 1.7 MPa. Greene derives Equation 3 more rigorously and reviews the literature to give a range of values for α, A, and the compliance of the eye (11).

Note that the ocular rigidity function really characterizes the properties of both the sclera and the cornea. Although the cornea is somewhat less stiff than the sclera (12–14), its elastic properties can also be described by a relationship analogous to Equation 2. Thus, Equation 3 actually describes the behavior of the corneoscleral envelope.

These formulations treat the sclera and cornea as elastic materials, but the ocular envelope also shows time-dependent deformations upon the application of stress. Viscoelastic models have been used to characterize this behavior (15–17), but, as in other tissues, a variety of time-constants are necessary to capture the behavior. This is likely due to the fact that the sclera is a biphasic material and thus better characterized by models that allow coupling of stresses with fluid motions in or out of the tissue (18, 19).

APPLICATIONS OF SCLERAL MECHANICS The most common use of the Friedenwald relationship is for tonometry (noninvasive measurement of IOP). There are different types of tonometers (20), the conceptually simplest of which is the Schiotz tonometer. This device measures the depth of indentation that occurs when a plunger of known weight is placed against the cornea. Gloster (21) summarized data for the relationship between intraocular pressure and the scale reading (for a given tonometer weight). However, this is the pressure in the eye with the tonometer distorting the eye. What is desired is the pressure of the undeformed eye. The indentation of the eye is equivalent to the injection of a fluid volume into the eye equal to the indentation volume. Gloster found a relationship between indentation depth and indentation volume of the tonometer. Then, using the Friedenwald relationship (Equation 1), the undeformed IOP can be found (22). This requires knowledge of the ocular rigidity, found either by using a population average or by using the Schiotz tonometer with two different plunger weights (22).

A related application of the Friedenwald relationship is in tonography in which a modified tonometer is used to estimate the aqueous humor drainage resistance in a live eye (23) (see also Aqueous Humor Dynamics, below). After the plunger increases the pressure in the eye, the pressure slowly decays as this indentation

volume flows out via the aqueous humor drainage pathway. By measuring the change in pressure over a short period of time (Δt, usually 4 min.), Equation 1 can be used to calculate the volume decrease of the corneoscleral envelope during this period (ΔV_s). Additionally, because the plunger indentation into the cornea increases as the pressure in the eye drops, this increased indentation volume (ΔV_c) must be included in the estimate of the total volume that has passed out of the eye. Then, outflow facility, C, the inverse of aqueous drainage resistance, can be estimated as $C = (\Delta V_s + \Delta V_c)/(\Delta t\ \Delta P)$, where ΔP is the average increase in IOP that occurred during the tonography. Greene (11) emphasized that ocular rigidity should be determined for a given eye before performing tonography, as very different results are expected for eyes of differing volumes (compare Equations 1 and 3 to see that K is inversely proportional to ocular volume). Note also that viscoelastic creep might confound the measurement of outflow facility by this method, but experimental studies indicate that this is not a serious error (24, 25).

Another important application of scleral mechanics is the understanding of myopia in which the axial length of the eye is too large to allow clear focussing of distant light rays on the retina. So far, we have considered the sclera to be a nonlinear elastic or viscoelastic material; however, the sclera has an elastic limit beyond which plastic deformation occurs (26, 27). Among the mechanical theories for explaining myopia, it has been postulated that these young eyes have (*a*) a genetically inherited decrease of this elastic limit, (*b*) higher than normal stresses on the sclera associated with accommodation and convergence that occur when reading (28), or (*c*) stretching caused by periodic increases in IOP owing to squinting or eye rubbing (27). It is possible that one or more of these mechanisms, combined with the physiological feedback loop responsible for growth of the eye (29–31), leads to the development of myopia.

Corneal Biomechanics

The cornea is a multilaminate tissue, consisting of an anterior stratified squamous "tight" epithelium (~50 microns thick), a tough collagenous stroma, and a posterior "leaky" monolayer of actively pumping endothelial cells (~5 microns thick). Its combination of remarkable strength and transparency is due to the highly organized micro- and nanoscale structure of the stroma (32, 33). On the microscale, the stroma comprises a nematic stack of 250–400 lamellae (34) containing type I/V heterotypic collagen fibrils (35). These fibrils run preferentially in the meridonal, horizontal, and (in the periphery) circumferential directions (36), and together help bear the load imposed by the IOP (Figure 2). In fact, the load may be taken up in a complex manner both in the plane of the cornea and transversely (37–40). Remarkably, there is no consensus on how the cornea is loaded in vivo. On the nanoscale, hydrophilic proteoglycans surround the 35-nm monodisperse collagen fibrils and impose a relatively uniform spacing on the collagen. The cornea's transverse material properties are determined primarily by the 36–48 mM of fixed charge density associated with the presence of these organizing proteoglycans (41, 42).

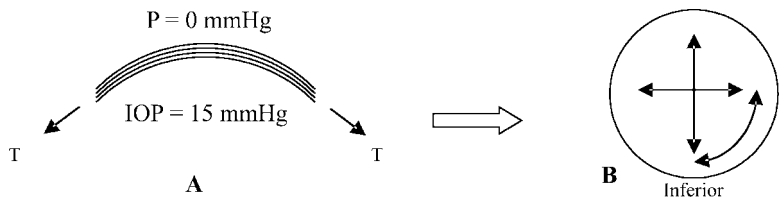

Figure 2 Corneal tensile load bearing. (*A*) Transverse view of cornea. Conversion of the 15 mmHg pressure difference across the cornea results in a tangential tensile force that is carried by the stromal lamellae. (*B*) En face view of cornea. Lamellar fibrils are thought to be oriented in three preferential orientations, which explains the anisotropic nature of the measured tensile modulus in the stroma.

MATERIAL PROPERTIES To generate a nearly perfectly spherical, aberration-free surface, the cornea must distribute applied loads with remarkable precision. To effect predictable shape changes to correct refractive errors, the corneal response to tissue resection/ablation must be characterized. Thus, it is of interest to discern the material properties of the cornea, which are heterogeneous, highly anisotropic, nonlinear, and viscoelastic. For example, for meridonal loading at normal IOP, Young's secant modulus is largest in the central cornea (8.6 MPa), whereas for circumferential loading, the secant modulus is largest in the periphery (13.0 MPa) (5). Woo et al. (4) used finite element analysis to obtain a nonlinear effective stress-strain relationship for clamped inflated human corneas of the form of Equation 2 with $A = 5.4 \times 10^4$ dyne/cm^2 and $\alpha = 28.0$. A more recent study of 12 human corneas found $A = 1.75 \times 10^4$ dyne/cm^2 and $\alpha = 48.3$ (43). Stress relaxation curves demonstrating the viscoelastic nature of peripheral corneal strips were fit with the following empirical equation (44):

$$y = -0.0159 \ln(t) + 0.9785, \tag{4}$$

where y is the normalized storage modulus at a fixed stretch ratio of 1.5 and t is time in seconds.

SWELLING PRESSURE In the anterior-posterior direction, the mammalian corneal stroma lacks internal mechanical constraints. The stroma therefore has a tendency to imbibe water, which is quantified through its "swelling pressure" (45). To prevent swelling, which leads to opacity, the cornea is compressed by the combined action of its limiting membranes (46), as discussed in detail in Transport Within the Cornea, below. Therefore, it is of interest to understand the magnitude and nature of the swelling forces that must be controlled to preserve vision. Stromal swelling pressure depends strongly on hydration (Figure 3), and can be described by (47)

$$p = \gamma \exp(-\beta H), \tag{5}$$

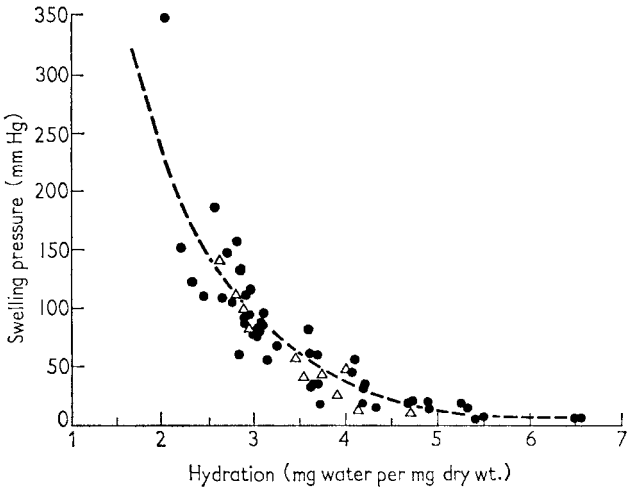

Figure 3 Swelling pressure in rabbit (*filled circles*) and human (*open triangles*) corneal stroma versus stromal hydration (mass water/mass dry tissue). The broken curve represents steer swelling pressure. At normal hydration (3.2–3.4 mg H_2O/mg dry material), this stromal swelling pressure is approximately 60 mmHg (52). From Hedbys & Dohlman (53).

where p is swelling pressure, γ and β are constants, and H is the hydration of the stromal tissue. Equation 5 is a regression of experimental data and tells us little about the physics of stromal swelling forces. Taking a more fundamental physical approach, Eisenberg & Grodzinsky (48, 49) extended KLM (50, 51) biphasic theory to include the effects of ionic species, expressing the swelling stress in the stroma, σ, as a function of the strain, ε, and the concentration of ionic species, c:

$$\sigma(c, \varepsilon) = E_A(c)\varepsilon + \sigma_c(c), \tag{6}$$

where E_A is the aggregate modulus [sum of the Lame's constants—2G(c) + λ(c)] and σ_c is the chemical stress. Eisenberg & Grodzinsky were able to extract both E_A and σ_c(c) as functions of c and use Equation 6 to predict the free swelling of the corneal stroma with reasonable accuracy (48).

APPLICATION TO REFRACTIVE SURGERY An obvious application of corneal biomechanics is to predict the laser ablation profile that will optimize postoperative visual acuity in refractive corneal procedures. However, biomechanical modeling has not been particularly successful in this task. Instead, laser manufacturers depend on continually updated, proprietary empirical algorithms (54) based on direct shape-subtraction (55) formulas that have been modified and statistically optimized to the mean patient population postoperative response (54). This empirical approach has been quite successful with up to 97% of the subjects willing to recommend LASIK (Laser ASsisted In-situ Keratomileusis) to a friend (56). How, then, did

the biomechanician fail, with the embarrassing result that human corneas became test cases for the development of a vast empirical database?

In spite of a sophisticated effort to model radial keratotomy (RK) refractive surgical outcomes during the late 1980s and early 1990s (57–61), the practical application of these models never really gained acceptance for four reasons: (*a*) Early RK models could not be validated (61); (*b*) the spatially variant mechanical properties of the stroma are not well defined on the relevant microscopic length scale (37); (*c*) the distribution of load in the stroma, which sets the local value of the nonlinear tensile modulus [to which refractive models are highly sensitive (43)] is not definitively known; and finally (*d*) the long-term stromal remodeling response is not addressed at all by mechanical models. These limitations, in combination with the undeniable effectiveness of the empirical approach, have virtually ensured that predictive biomechanical modeling of refractive procedures is not likely to enjoy resurgent popularity in the near future. In a further ironic twist, topographic corneal maps obtained following laser ablation surgeries are being used to "back out" information about stromal structure and material properties (54).

Retina and Lamina Cribrosa Biomechanics

The retina is a remarkably fragile tissue, having a thickness of 250 μm (62) and a Young's modulus of only 20 kPa (63). It does not carry significant load, but it can tear, usually with drastic visual consequences. Retinal tears are often associated with age-related liquefaction and shrinkage of the vitreous body (64), but can also occur when the eye is subjected to large accelerations (65), such as in shaken baby syndrome (66).

The lamina cribrosa is one of the most biomechanically interesting tissues in the eye. It is a porous connective tissue that spans the scleral canal, mechanically supporting the retinal ganglion cells of the optic nerve as they pass through the scleral canal. The lamina cribrosa is very important in glaucoma, a group of diseases having a common clinical end point of visual field loss and characteristic changes to the optic nerve. Glaucoma is the second most common cause of blindness in western countries and afflicts approximately 65 to 70 million people worldwide (67). In the most common forms of glaucoma, IOP is elevated (to 21 mmHg or higher), and if this elevated IOP is sustained, retinal ganglion cell loss ensues and blindness eventually results. We do not yet completely understand the mechanism of ganglion cell loss, but studies have strongly suggested that the lamina cribrosa is the site of damage (68–70). This has led to the mechanical theory of glaucomatous optic neuropathy, which postulates that elevated mechanical stresses acting within the lamina cribrosa lead to nerve fiber damage, probably through activation of Type 1-β astrocytes and/or other glial cells (71). Such mechanical effects may combine synergistically with altered vascular perfusion in the optic nerve head to damage retinal ganglion cells (see Blood Flow in the Eye, below).

In order to evaluate the possible role of mechanical stress in glaucoma, we must know something about the mechanical environment within the lamina cribrosa. Unfortunately, the lamina cribrosa is small, relatively inaccessible, soft, and

surrounded by a much stiffer tissue (sclera). This makes experiments challenging, and most measurements have relied on post mortem histologic examination (72, 73), or other indirect measurements of deformation (74–76). Others have adopted a modeling approach, treating the lamina as a circular plate of finite thickness (77, 78). Unfortunately, the lamina is much more geometrically complex than such analytic treatments allow, and thus numerical modeling is an attractive option. Bellezza et al. (79) considered a simplified model of the lamina cribrosa consisting of regular networks of connective tissue "bridges" spanning an elliptical scleral canal. Their results showed remarkable stress elevations in the lamina cribrosa bridges, in some cases more than 100 times the applied IOP. Sigal et al. (80), also using a finite element approach, modeled the sclera, lamina cribrosa, and pre- and postlaminar nerve tissue, finding von Mises strains of up to 12% within the lamina at an IOP of 50 mmHg. Such models are relatively crude at present, assuming linear elasticity, tissue isotropy, and simplified geometries. Nonetheless, when supported by suitable experimental studies, they are a promising tool for unraveling the mysteries of lamina cribrosa biomechanics in glaucoma.

Accommodation and Presbyopia

Although there are many changes that occur with aging, perhaps the most universal is the loss of the ability to accommodate, i.e., to change the focal length of the eye by changing lens shape. This condition is known as presbyopia, familiar to everyone who has purchased a pair of reading glasses, and typically begins during the fifth decade of life. Several hypotheses have been offered for the causes of presbyopia, including (*a*) a decreased elasticity of the lens, making it more resistant to deformation; (*b*) changes in the geometry of the anterior segment and the lens, resulting in a loss of mechanical effectiveness of zonular tightening; and (*c*) loss of ciliary muscle contractility.

There appears to be good evidence supporting all of these hypotheses. The lens definitely becomes stiffer with age (81–83). There are changes in the geometry of the anterior segment, including an anterior motion of the lens and of the ciliary muscle, an increased size and curvature of the lens, and a decreased anterior chamber depth (84). Other studies (85, 86) have shown that although the ciliary muscle loses its ability to contract in older individuals, the muscle itself is not weakened (87, 88) and remains sensitive to cholinergic agonists (89). Recent evidence indicates that changes in the connective tissues around the ciliary muscle may inhibit its ability to freely contract (90). Thus, the pathophysiology of presbyopia may be multifactorial.

OCULAR BIOFLUID MECHANICS AND TRANSPORT

Blood flows through the eye, aqueous humor is produced within and drains from the eye, and interstitial fluid percolates through connective tissues within the eye. These myriad fluid pathways contain many fascinating and challenging biomechanical problems.

Blood Flow in the Eye

All blood is supplied to the eye by the ophthalmic artery. The eye has two main vascular systems: the retinal and uveal. The retinal circulation is fed and drained by the central retinal artery and vein, both of which enter the eye through the scleral canal. The retinal circulation is responsible for supplying blood to the inner retina and is autoregulated (91, 92) so that it provides a nearly constant blood flow rate even as IOP increases up to 30 mmHg. Above this pressure, blood flow is reduced as IOP increases. As the blood flow to the inner aspects of the optic nerve head is also served by the retinal circulation (91), this may have some importance in glaucoma.

The uveal circulation can itself be divided into two parts. The anterior uveal circulation is responsible for supplying blood to vascular tissues of the anterior eye, in particular the iris and ciliary body, where it is involved in the formation of the aqueous humor (see Aqueous Humor Dynamics, below). The iridial circulation is autoregulated (91). The posterior uveal circulation feeds a specialized vascular bed known as the choroid, lying between the retina and sclera. The choroid supplies blood to the outer retina, which has a very high metabolic rate (93). In fact, the choroidal flow is the highest flow per perfused volume of any tissue in the body (8), with approximately 85% of total ocular blood flow passing through the choroid (91). Because the oxygen needs of even the retina are greatly exceeded by this supply (91), the reason for such a high perfusion rate is not known, although a number of creative hypotheses have been offered (94–97). The choroidal flow is thought not to be autoregulated (91), but there is some recent evidence to the contrary (98, 99). The uveal circulation is drained by a venous system consisting of two parts (100). Most blood drains through the vortex veins, four large veins (in the human) that exit the eye through the posterior sclera. The anterior ciliary veins drain part of the ciliary muscle.

The physiology of blood flow in the eye, particularly on the venous side, is strongly influenced by IOP. In most of the circulatory system, flow is determined by the difference between the arterial and venous pressures. However, in the eye, the perfusion pressure is the difference between the arterial pressure and IOP. This relates to the well-known problem of flow through collapsible tubes under the influence of an external pressure (101–103). When the external pressure surrounding a blood vessel is greater than the pressure within that vessel, the vessel collapses, initially at the distal end of the vessel, where the pressure is lowest. As this constriction is the location where most of the pressure drop occurs, upstream of this collapse region the pressure in the vessel is at least equal to the external pressure. Thus, while the arterial pressure in the eye is somewhat lower than in the rest of the body [in the uvea, 75 mmHg systolic and 35 mmHg diastolic (104)], venous pressure in the eye (other than in the sclera) is always above 15 mmHg. Pressures in the choriocapillaris are typically 5–10 mmHg higher than IOP (100).

The region of vessel collapse occurs in the veins as they pass from the vitreous chamber into the sclera. This collapse is necessary for the pressure in the vessel to drop from IOP to episcleral venous pressure [typically 8–10 mmHg in the eye (105,

106)]. The dramatic change in the vessel cross-section that occurs at this point is known as a vascular waterfall. It is a point of flow limitation, similar to what occurs at the nozzle throat in supersonic flow, or at a waterfall (102). In all of these flows, once the flow velocity has reached the wave speed at the point of flow limitation, the flow becomes insensitive to the downstream pressure. The consequence is that, as indicated above, ocular blood flow is very sensitive to the IOP. This is likely the reason why several of the circulations in the eye are autoregulated. It is also the basis for the theory that glaucomatous damage to the optic nerve is caused by reduced blood flow owing to the elevated IOP (107).

Aqueous Humor Dynamics

For proper visual acuity the eye must be relatively rigid, yet the mammalian eye contains no bones. How then is rigidity maintained? Further, the lens and cornea must remain clear to allow light transmission, and therefore cannot be invested with a vasculature. How then are the cells nourished in these tissues? The eye has solved both problems with a common (and clever) mechanism: The corneoscleral shell is inflated by the production and drainage of the aqueous humor, which also serves to nourish the lens and cornea. The best analogy is a soccer ball with a slow leak whose air is constantly being replenished from a pump. The aqueous humor can also clear debris from within the eye, e.g., red cells from intraocular haemorrhage.

The aqueous humor is produced at 2.4 ± 0.6 μl/min (mean $\pm$ SD, daytime measurements in adults aged 20–83 years) (108). This corresponds to a turnover rate of 1% of the anterior chamber volume per minute, i.e., relatively slowly. Aqueous humor production varies diurnally: It is normally about 3.0 μl/min in the morning, 2.4 μl/min in the afternoon, and drops to 1.5 μl/min at night (108). It is produced primarily by active transport across epithelial cells lining the surface of the ciliary processes (109), and the rate of production is relatively independent of IOP.

The aqueous humor drains from the eye via two routes, the so-called conventional and uveo-scleral (or unconventional) routes. Uveo-scleral outflow normally carries only approximately 10% of total outflow (110, 111); we consider it again in Scleral Permeability and Drug Delivery to the Eye, below. Most aqueous humor instead drains via specialized tissues situated in the angle of the anterior chamber, located at the conjunction of the iris, cornea, and sclera. Beginning at the anterior chamber and moving exteriorly, these tissues are the trabecular meshwork, a porous connective tissue; Schlemm's canal, a collecting duct lined by a vascular-like endothelium; and the collector channels/aqueous veins. Direct pressure measurements (112, 113) and circumstantial evidence (114) indicate that most of the flow resistance in the normal nonglaucomatous eye is in the juxtacanalicular tissue (JCT) or the endothelial lining of Schlemm's canal. After leaving the aqueous veins, the aqueous humor mixes with blood in the episcleral veins, eventually draining back to the right heart (Figure 4). The episcleral venous pressure is approximately 8–10 mmHg (105, 106), and the resistance of the

conventional aqueous drainage tissues is approximately 3–4 mmHg/μl/min, resulting in an IOP of 15.5 $\pm$ 2.6 mmHg (mean $\pm$ SD) in the general population (115).

This would be an interesting curiosity if it were not for the problem of glaucoma. We know that elevated IOP is the main risk factor for glaucoma, and that lowering IOP helps preserve visual function (116). In the vast majority of glaucomas, the elevation in IOP is due to too much aqueous humor drainage resistance, and in the majority of these cases the elevated resistance is due to pathologic changes in the conventional drainage tissues. Despite years of intensive research, we understand little of how aqueous drainage resistance is controlled in normal and glaucomatous eyes.

One of the big questions in glaucoma research is: Where is the aqueous flow resistance? Models of Schlemm's canal as a compliant chamber with a porous, elastic wall suggest negligible flow resistance within the canal itself, except at extreme intraocular pressures (>50 mmHg) when the canal collapses (117). Known concentrations of proteoglycan-rich gels within the extracellular spaces of the juxtacanalicular tissue are consistent with the generation of significant flow resistance (118); recent data suggest that the turnover of this matrix is modulated by stretch-induced matrix metalloproteinases (MMP) activity within the trabecular meshwork (119–121). However, the evidence supporting a primary role for extracellular matrix is far from iron-clad (see review in 122), and researchers have looked elsewhere. The other "candidate" for generating flow resistance is the endothelial lining of Schlemm's canal. This cellular layer is unusual; for example, it has the highest permeability of any endothelium (123), with $L_p \geq 4 \times 10^{-8}$ cm^2 s/g, yet it is nonfenestrated (but see below). The cells are joined by tight junctions that become less tight as IOP increases (124) and are permeated by membrane-lined openings (pores) that, although poorly understood, are almost certainly involved in aqueous humor transport (125). The pores represent only approximately 0.1% of the total endothelial area and have a mean diameter just slightly over 1 μm (125). A model of the pores in the endothelial lining modulating the flow through a porous juxtacanalicular tissue (127) suggests that overall flow resistance may depend on an interaction between the endothelial pores and extracellular matrix.

The endothelial cells lining Schlemm's canal bulge prominently into the lumen of the canal, forming the so-called giant vacuoles. Evidence suggests these are passive structures that form in response to the "backward" basal-to-apical pressure gradient that is always present across the cells (128, 129). The extreme case is when you rub your eyes, instantaneously generating pressures as high as 80 mmHg (130)! These large IOPs form so many giant vacuoles that inner wall endothelial cells may stretch by as much as 50% (131), a harsh biomechanical environment indeed.

The biomechanics of aqueous humor flow within the anterior chamber are also interesting. Because the cornea is normally exposed to ambient air, the temperature at the posterior corneal surface is slightly less than body temperature, thus creating a temperature gradient across the anterior chamber. The resulting convection patterns (132, 133) tend to transport particles in vertical paths along the mid-peripheral

cornea (Figure 4). The clinical correlate of this effect is pigment particles that are seen to accumulate along such paths in patients whose irises release abnormal amounts of pigments.

There is a form of glaucoma in which the elevated IOP is not due to changes in the drainage system of the eye per se. This is angle-closure glaucoma, when the iris pivots forward and blocks access to the drainage structures in the angle of the anterior chamber. There appears to be an anatomic predisposition to this situation. The iris is extremely pliable (134), and modeling has shown interesting interactions between iris deformation and aqueous flow through the pupil and between the lens and the iris, especially when the eye is perturbed by blinking (135, 136).

Transport Within the Cornea

To maintain transparency, the corneal stroma must be prevented from swelling. The flows and forces that nourish and deturgesce the stroma are subtle and complex. Although there is some evidence for limbally derived lateral flow (137, 138) because of the 10:1 ratio of lateral to transverse diffusion distance, the corneal transport system is essentially one-dimensional in the AP (anterior-to-posterior) direction (Figure 5). To understand this AP transport, we must consider the role of the corneal membranes. The epithelium, with its complete tight junctions, primarily protects the stroma [although it does have some limited active pumping ability (139)], whereas the endothelium, with its incomplete tight junctions and its plethora of basolateral ATPases, removes fluid yet allows free diffusion of nutrients and cytokines from the aqueous humor (46). Globally, there is approximately a 20 micron/h net flow velocity out of the cornea to the tear film, driven by the transcorneal pressure gradient and by evaporation from the tear film (140). Intriguingly, however, the corneal endothelium can generate a fluid velocity of 40 microns/h in the opposite direction, effectively compressing the stroma (141).

Fluid transport through the cornea depends on the hydraulic permeabilities, L_p, of the endothelium, epithelium, and stroma. Isolating functioning membranes from

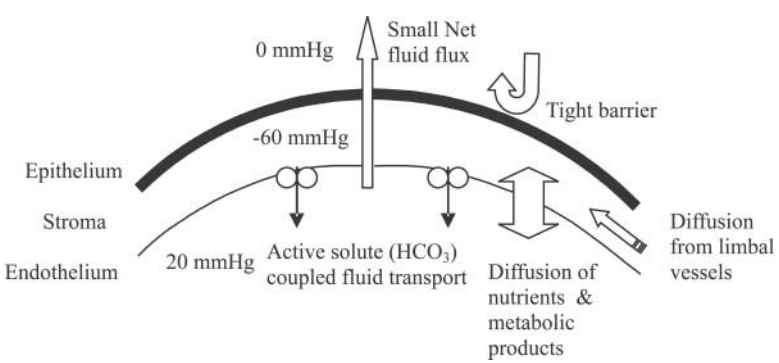

Figure 5 Key elements of the corneal transport system.

the hydrophilic stroma to measure L_p is not feasible. However, Klyce & Russell (142) were able to extract L_p for both the endothelium (42.0×10^{-12} cm^3/dyne sec) and the epithelium (6.1×10^{-12} cm^3/dyne sec) by coupling thermodynamic representations of the membranes (143) to a dynamic stromal transport model (47) and fitting the model to the corneal response to osmotic challenges. As expected, the endothelium is more permeable to water than the epithelium (by a factor of seven). From the same series of experiments, the ratio of endothelial to epithelial NaCl permeability was much larger than one as well. To produce dynamic corneal transport models (e.g., 142), it is necessary to know the value of stromal hydraulic conductivity, k/η, as a function of tissue hydration. The elegant work of Hedbys & Mishima (144) relates the stromal hydraulic conductivity in both the in-plane and transverse direction to hydration (Figure 6).

Typically, stromal fluid transport and hydraulic conductivity have been measured on bulk tissue. Recently, however, Ruberti et al. (145) tracked microscale

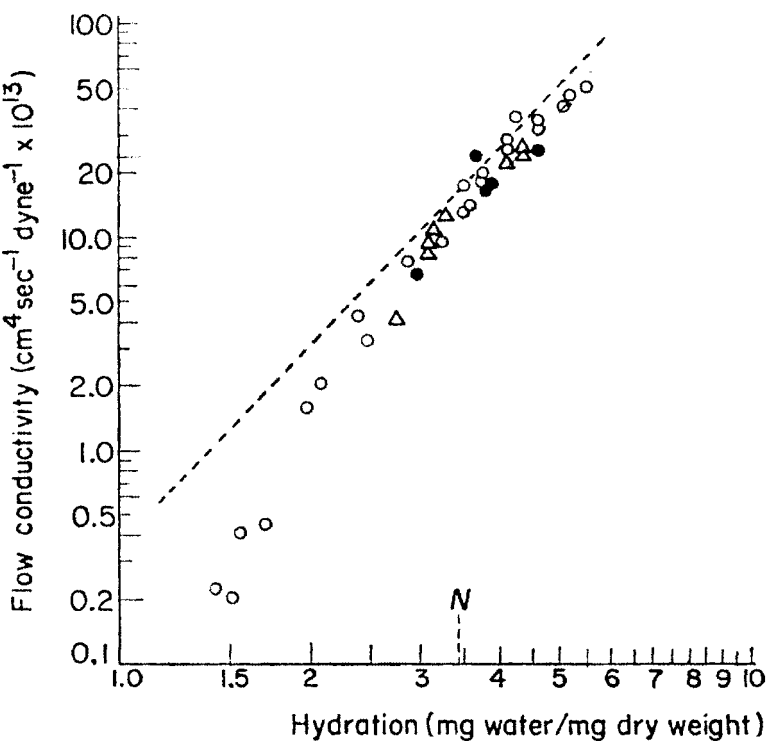

Figure 6 Flow conductivity versus hydration across the cornea. The symbols refer to measurements taken with (*closed circles*) and without (*open circles*) Descemet's membrane in 0.9% NaCl, or without Descemet's membrane in distilled water (*triangles*). The broken line represents the flow conductivity versus hydration relationship for flow along the cornea. N is the normal corneal hydration. From Hedbys & Mishima (144).

intrastromal flows in response to corneal debridement, and Overby et al. (146) determined intrastromal specific hydraulic conductivity directly from structure-preserving micrographs. Such investigations promise to improve our understanding of microscale corneal transport dynamics.

Transport Across Bruch's Membrane

In addition to the corneal endothelium, there are several sites of active transport in the eye, including the ciliary epithelium, responsible for production of aqueous humor, and the retinal pigment epithelium (RPE), which removes fluid from the retina and thus helps keep the retina attached (147–149).

The RPE rests on a basement membrane that is part of Bruch's membrane, a five-layer barrier structure that limits transport between the choroid and the outer retina. These five layers, beginning at the RPE and proceeding outward toward the choroid, are the basement membrane of the RPE, the inner collagenous layer, the elastin layer, the outer collagenous layer, and the basement membrane of the choriocapillaris (150). Oxygen, electrolytes, nutrients, and cytokines from the choroidal circulation must pass through this barrier to reach the retina, whereas waste products from the retina and water pumped by the RPE must pass back through this barrier to be eliminated into the blood stream.

Water transport through this membrane is the best studied of these transport processes. After the RPE pumps water from the retinal space into Bruch's membrane, the water moves under the influence of both hydrostatic and osmotic pressure gradients into the choroidal circulation (91, 151). The hydraulic resistance of Bruch's membrane increases with age (Figure 7). This increase has been hypothesized to contribute to the pathology of age-related macular degeneration (AMD) by inhibiting fluid transport by the RPE and consequently causing retinal detachment (152).

The age-related increase in the hydraulic resistance of Bruch's membrane is thought to be a consequence of lipid accumulation (153) because the age-related increase in resistance parallels the age-related accumulation of lipid in Bruch's membrane (Figure 7). These lipids may originate as waste products from the retina that are processed by the RPE (154).

It has been shown that there is a parallel age-related increase in the transport resistance of Bruch's membrane to protein transport (156), although that study may not have properly accounted for osmotic effects of the proteins examined. Little study has yet been done on the transport of other moieties across Bruch's membrane.

Scleral Permeability and Drug Delivery to the Eye

Drug delivery to intraocular tissues is important in treating a variety of ocular diseases. Systemic administration of these agents is undesirable because it necessitates high plasma concentrations to achieve adequate intraocular dosing. Transcorneal delivery by passive diffusion is difficult because the drug needs to have

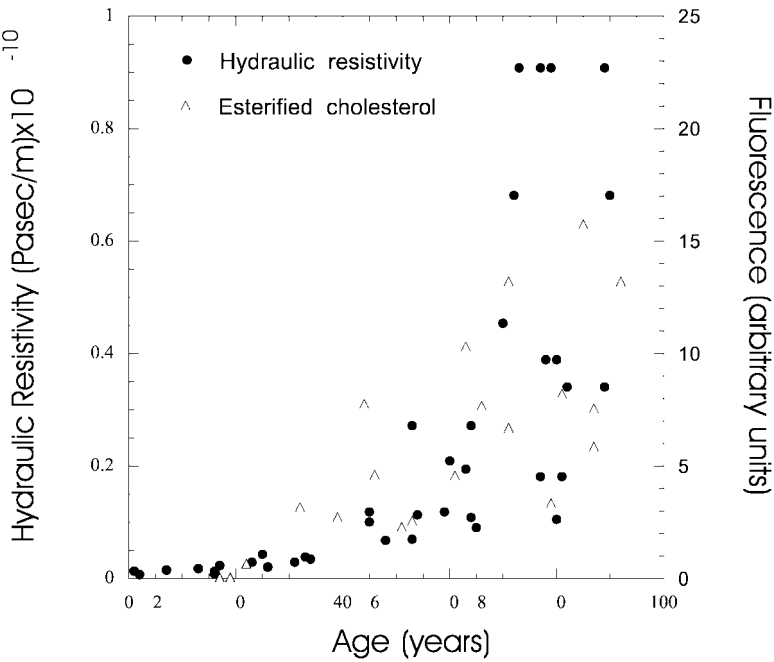

Figure 7 Hydraulic resistivity (150) of excised Bruch's membrane/choroid (*closed symbols*) and fluorescence owing to histochemically detected esterified cholesterol in sections of normal Bruch's membrane (155) (*open symbols*) as a function of age.

hydrophobic characteristics to pass through the corneal epithelium and endothelium, and hydrophilic characteristics to pass through the corneal stroma. Furthermore, as soon as the agent enters the anterior chamber, it is carried out of the eye by the aqueous humor. Scleral delivery, especially for drugs destined for the retina (157), may be a more attractive route for drug administration (158), as the tight epithelial barriers of the cornea are not present on the sclera (159). However, the scleral stroma is still a significant barrier, and a number of studies have examined the permeability of this tissue.

As expected, scleral permeability to solute transport decreases with increasing solute molecular weight and increasing molecular radius, with the latter a better predictor of scleral permeability than the former (160). The posterior sclera is more permeable to solute transport than the anterior sclera, further supporting the sclera as an ideal route for drug delivery to the retina (161).

The specific hydraulic conductivity of the sclera is 2×10^{-14} cm^2, typical of dense connective tissues (162). With a typical pressure difference across the sclera of 15 mmHg; a scleral thickness, L, of 0.6 mm (163); and a filtering area, A, of 11.5 cm^2 [the total scleral area (163)], we can use Darcy's law to estimate a

maximum flow rate (Q) across the sclera of 0.3 μl/min. The flow rate can be used to examine several issues related to fluid flow though the scleral stroma.

The first question is the extent to which this flow impedes drug delivery across the sclera. The diffusional flux of a drug through a tissue can be estimated as

$$D_0(1 - \Phi)A\frac{\Delta C}{L}, \tag{7}$$

whereas the convective flux of a drug through that same tissue would be

$$QC(1 - \Phi). \tag{8}$$

Here D_0 is the diffusion coefficient of the tracer in free solution (for albumin 6×10^{-7} cm^2/sec); Φ is the extent to which the tracer is retarded, relative to the fluid flow, from moving by the extracellular matrix (0 is unhindered, 1 completely hindered); and ΔC is the concentration difference across the sclera, which we assume is the same as the concentration of drug at the surface of the sclera. Using these formulas, the ratio of diffusional transport to convective transport is computed to be approximately 20 for molecules the size of albumin. In other words, for these parameters, diffusional transport of a drug across the sclera is more than an order-of-magnitude higher than transport of the drug by convection. Thus, bulk flow across the sclera should have minimal impact on drug delivery through the sclera.

We can also use the value of Q to gain insight into the unconventional drainage pathway (Aqueous Humor Dynamics, above) that normally carries a small fraction of the aqueous humor from the eye. Aqueous humor draining via this pathway passes through the ciliary muscle, into the suprachoroidal space, and then passes (*a*) either through the sclera into the orbit or (*b*) through the sclera to the vortex veins and choroidal circulation, where it is absorbed. Arguments have been provided for each of these pathways (123, 164, 165). The value of Q calculated above as 0.3 μl/min would appear to support the former pathway because this value is consistent with measured values of unconventional aqueous outflow rates (166). However, it is known that ciliary muscle contraction greatly affects the unconventional outflow (167), and that $PGF_{2\alpha}$ greatly increases unconventional outflow by decreasing the flow resistance of the interstitial spaces in the ciliary muscle (168, 169). This can only be the case if the flow resistance of the ciliary muscle is of the same order of magnitude or even larger than that of the sclera; otherwise, changes in the muscle would make little difference. But, in that case, the calculated flow rate of 0.3 μl/min must be an upper bound that does not consider the flow resistance of the ciliary muscle. A further argument against a trans-scleral flow is that unconventional outflow is not very pressure sensitive (170). Although this might be expected if the flow were primarily osmotically driven into the uveal vessels, this would not be the expected characteristic of a trans-scleral flow. Each of these considerations argue against trans-scleral flow, but are consistent with osmotic adsorption of the unconventional aqueous outflow by the choroidal circulation (123).

SUMMARY AND OPEN PROBLEMS

From this brief summary it is clear that there is a great deal of interesting biomechanics in the eye. We are far from understanding all the relevant biomechanics in this understudied field, and hence we close with a list of open problems to tempt researchers.

- Why does presbyopia occur? There have been no biomechanical modeling studies that account for all of the physiological observations mentioned in Accommodation and Presbyopia (above) and attempt to comprehensively evaluate the mechanisms underlying presbyopia. More generally, fundamental studies about the biomechanics of accommodation are also needed.
- How is outflow resistance generated in the normal eye, and what goes wrong to increase this resistance in most forms of glaucoma?
- How does elevated IOP damage the optic nerve and lead to blindness in glaucoma?
- What are the biomechanics of myopia?
- How can we determine microscale material properties and corneal stress field noninvasively, in vivo? If this can be accomplished, then the biomechanicist might provide input for refractive corneal surgery on a case-by-case basis.
- How is the hydration of the cornea controlled? No control signal has been identified to date, yet corneas maintain their hydration in a relatively tight range. Recently, Ruberti & Klyce (171) demonstrated that 5% changes in NaCl concentration induced compensatory changes in endothelial pump rate, suggesting a possible homeostatic response triggered by NaCl.

ACKNOWLEDGMENTS

Our work has benefited from ongoing grant support from the Canadian Institutes of Health Research (CRE), the Glaucoma Research Society of Canada (CRE), International Retinal Research Foundation (MJ), the American Health Assistance Foundation (MJ), and the National Institutes of Health (R01 EY014662; MJ).

The *Annual Review of Biomedical Engineering* is online at http://bioeng.annualreviews.org

LITERATURE CITED

1. Demer JL. 2002. The orbital pulley system: a revolution in concepts of orbital anatomy. *Ann. NY Acad. Sci.* 956:17–32
2. Krey HF, Bräuer H. 1998. *Chibret Augenatlas: Eine Repetition für Ärtze mit Zeigetafeln für Patienten*. Munich: Chibret Med. Serv.
3. Jue B, Maurice DM. 1986. The mechanical properties of the rabbit and human cornea. *J. Biomech.* 19:847–53

4. Woo SL, Kobayashi AS, Schlegel WA, Lawrence C. 1972. Nonlinear material properties of intact cornea and sclera. *Exp. Eye Res.* 14:29–39
5. Hjortdal JO. 1996. Regional elastic performance of the human cornea. *J. Biomech.* 29:931–42
6. Battaglioli JL, Kamm RD. 1984. Measurements of the compressive properties of scleral tissue. *Invest. Ophthalmol. Vis. Sci.* 25:59–65
7. Friedenwald JS. 1937. Contribution to the theory and practice of tonometry. *Am. J. Ophthalmol.* 20:985–1024
8. Collins R, van der Werff TJ. 1980. Mathematical models of the dynamics of the human eye. In *Lecture Notes in Biomathematics*. Berlin: Springer-Verlag
9. Fung YC. 1967. Elasticity of soft tissues in simple elongation. *Am. J. Physiol.* 213:1532–44
10. McEwen WK, St Helen R. 1965. Rheology of the human sclera. Unifying formulation of ocular rigidity. *J. Biol. Chem.* 240:2003–10
11. Greene PR. 1985. Closed-form ametropic pressure-volume and ocular rigidity solutions. *Am. J. Optom. Physiol. Opt.* 62:870–78
12. Woo SL, Kobayashi AS, Schlegel WA, Lawrence C. 1972. Nonlinear material properties of intact cornea and sclera. *Exp. Eye Res.* 14:29–39
13. Woo SL-Y, Kobayashi AS, Lawrence C, Schlegel WA. 1972. Mathematical model of the corneo-scleral shell as applied to intraocular pressure-volume relations and applanation tonormetry. *Ann. Biomed. Eng.* 1:87–98
14. Nash IS, Greene PR, Foster CS. 1982. Comparison of mechanical properties of keratoconus and normal corneas. *Exp. Eye Res.* 35:413–24
15. Lyon C, McEwen WK, Shepherd MD. 1970. Ocular rigidity and decay curves analyzed by two nonlinear systems. *Invest. Ophthalmol. Vis. Sci.* 9:935–45
16. St. Helen R, McEwen WK. 1961. Rheology of the human sclera. I. Anelastic behavior. *Am. J. Ophthalmol.* 52:539
17. Downs JC, Suh JK, Thomas KA, Bellezza AJ, Burgoyne CF, Hart RT. 2003. Viscoelastic characterization of peripapillary sclera: material properties by quadrant in rabbit and monkey eyes. *J. Biomech. Eng.* 125:124–31
18. Mow VC, Holmes MH, Lai WM. 1984. Fluid transport and mechanical properties of articular cartilage: a review. *J. Biomech.* 17:377
19. Johnson M, Tarbell JM. 2001. A biphasic, anisotropic model of the aortic wall. *J. Biomech. Eng.* 123:52–57
20. McDermott JA. 1989. Tonography. See Ref. 172, pp. 293–99
21. Gloster J. 1965. Tonometry and tonography. *Int. Ophthalmol. Clin.* 5:911–1133
22. Fatt I. 1978. *Physiology of the Eye: An Introduction to the Vegetative Functions*. Boston, MA: Butterworth
23. Grant WM. 1950. Tonographic method for measuring the facility and rate of aqueous flow in human eyes. *Arch. Ophthalmol.* 44:204–14
24. Viernstein LJ, Kitazawa Y. 1970. Measurements of factors affecting the precision of tonometry and tonography. *Exp. Eye Res.* 9:91–97
25. Viernstein LJ, Cowan M. 1969. Static and dynamic measurements of the pressure-volume relationship in living and dead rabbit eyes. *Exp. Eye Res.* 8:183–92
26. Greene PR, McMahon TA. 1979. Scleral creep vs. temperature and pressure in vitro. *Exp. Eye Res.* 29:527–37
27. Ku DN, Greene PR. 1981. Scleral creep in vitro resulting from cyclic pressure pulses: applications to myopia. *Am. J. Optom. Physiol. Opt.* 58:528–35
28. Greene PR. 1980. Mechanical considerations in myopia: relative effects of accommodation, convergence, intraocular pressure, and the extraocular muscles. *Am. J. Optom. Physiol. Opt.* 57:902–14
29. Wiesel TN, Raviola E. 1977. Myopia and

eye enlargement after neonatal lid fusion in monkeys. *Nature* 266:66–68
30. Wallman J, Turkel J, Trachtman J. 1978. Extreme myopia produced by modest change in early visual experience. *Science* 201:1249–51
31. Goss DA, Wickham MG. 1995. Retinal-image mediated ocular growth as a mechanism for juvenile onset myopia and for emmetropization. A literature review. *Doc. Ophthalmol.* 90:341–75
32. Maurice D. 1957. The structure and transparency of the cornea. *J. Physiol.* 136:263–86
33. Goldman JN, Benedek GB. 1967. The relationship between morphology and transparency in the nonswelling corneal stroma of the shark. *Invest. Ophthalmol. Vis. Sci.* 6:574–600
34. Pouliquen Y. 1985. Fine structure of the corneal stroma. *Cornea* 3:168–77
35. Birk DE, Fitch JM, Babiarz JP, Linsenmayer TF. 1988. Collagen type I and type V are present in the same fibril in the avian corneal stroma. *J. Cell Biol.* 106:999–1008
36. Meek KM, Fullwood NJ. 2001. Corneal and scleral collagens—a microscopist's perspective. *Micron* 32:261–72
37. Shin TJ, Vito RP, Johnson LW, McCarey BE. 1997. The distribution of strain in the human cornea. *J. Biomech.* 30:497–503
38. Waring GO 3rd. 1999. A cautionary tale of innovation in refractive surgery. *Arch. Ophthalmol.* 117:1069–73
39. McPhee TJ, Bourne WM, Brubaker RF. 1985. Location of the stress-bearing layers of the cornea. *Invest. Ophthalmol. Vis. Sci.* 26:869–72
40. Hennighausen H, Feldman ST, Bille JF, McCulloch AD. 1998. Anterior-posterior strain variation in normally hydrated and swollen rabbit cornea. *Invest. Ophthalmol. Vis. Sci.* 39:253–62
41. Hodson S, O'Leary D, Watkins S. 1991. The measurement of ox corneal swelling pressure by osmometry. *J. Physiol.* 434:399–408
42. Otori T. 1967. Electrolyte content of the rabbit corneal stroma. *Exp. Eye Res.* 6:356–67
43. Bryant MR, McDonnell PJ. 1996. Constitutive laws for biomechanical modeling of refractive surgery. *J. Biomech. Eng.* 118:473–81
44. Zeng Y, Yang J, Huang K, Lee Z, Lee X. 2001. A comparison of biomechanical properties between human and porcine cornea. *J. Biomech.* 34:533–37
45. Flory PJ. 1953. *Principles of Polymer Chemistry*. Ithaca, NY: Cornell Univ. Press. 672 pp.
46. Maurice DM. 1984. The cornea and sclera. In *The Eye*, ed. H Davson. New York: Academic
47. Fatt I, Goldstick T. 1965. Dynamics of water transport in swelling membranes. *J. Colloid Sci.* 20:962–89
48. Eisenberg SR, Grodzinsky AJ. 1985. Swelling of articular cartilage and other connective tissues: electromechanochemical forces. *J. Orthop. Res.* 3:148–59
49. Eisenberg SR, Grodzinsky AJ. 1987. The kinetics of chemically induced nonequilibrium swelling of articular cartilage and corneal stroma. *J. Biomech. Eng.* 109:79–89
50. Myers ER, Lai WM, Mow VC. 1984. A continuum theory and an experiment for the ion-induced swelling behavior of articular cartilage. *J. Biomech. Eng.* 106:151–58
51. Mow VC, Kuei SC, Lai WM, Armstrong CG. 1980. Biphasic creep and stress relaxation of articular cartilage in compression? Theory and experiments. *J. Biomech. Eng.* 102:73–84
52. Hedbys B, Mishima S, Maurice D. 1963. The imbibition pressure of the corneal stroma. *Exp. Eye Res.* 2:99–111
53. Hedbys B, Dohlman C. 1963. A new method for the determination of the swelling pressure of the corneal stroma in vitro. *Exp. Eye Res.* 2:122–29
54. Roberts C. 2000. The cornea is not a piece of plastic. *J. Refract. Surg.* 16:407–13

55. Munnerlyn CR, Koons SJ, Marshall J. 1988. Photorefractive keratectomy: a technique for laser refractive surgery. *J. Cataract. Refract. Surg.* 14:46–52
56. Bailey MD, Mitchell GL, Dhaliwal DK, Boxer Wachler BS, Zadnik K. 2003. Patient satisfaction and visual symptoms after laser in situ keratomileusis. *Ophthalmology* 110:1371–78
57. Hanna KD, Jouve FE, Waring GO 3rd. 1989. Preliminary computer simulation of the effects of radial keratotomy. *Arch. Ophthalmol.* 107:911–18
58. Pinsky PM, Datye DV. 1991. A microstructurally-based finite element model of the incised human cornea. *J. Biomech.* 24:907–22
59. Velinsky SA, Bryant MR. 1992. On the computer-aided and optimal design of keratorefractive surgery. *Refract. Corneal. Surg.* 8:173–82
60. Vito RP, Shin TJ, McCarey BE. 1989. A mechanical model of the cornea: the effects of physiological and surgical factors on radial keratotomy surgery. *Refract. Corneal. Surg.* 5:82–88
61. Wray WO, Best ED, Cheng LY. 1994. A mechanical model for radial keratotomy: toward a predictive capability. *J. Biomech. Eng.* 116:56–61
62. Alamouti B, Funk J. 2003. Retinal thickness decreases with age: an OCT study. *Br. J. Ophthalmol.* 87:899–901
63. Jones IL, Warner M, Stevens JD. 1992. Mathematical modelling of the elastic properties of retina: a determination of Young's modulus. *Eye* 6(Pt. 6):556–59
64. Stevens JD, Jones IL, Warner M, Lavin MJ, Leaver PK. 1992. Mathematical modelling of retinal tear formation: implications for the use of heavy liquids. *Eye* 6(Pt. 1):69–74
65. David T, Smye S, Dabbs T, James T. 1998. A model for the fluid motion of vitreous humour of the human eye during saccadic movement. *Phys. Med. Biol.* 43:1385–99
66. Levin AV. 2002. Ophthalmology of shaken baby syndrome. *Neurosurg. Clin. N. Am.* 13:201–11, vi
67. Quigley HA. 1996. Number of people with glaucoma worldwide. *Br. J. Ophthalmol.* 80:389–93
68. Quigley HA, Addicks EM, Green WR, Maumenee AE. 1981. Optic nerve damage in human glaucoma; II: the site of injury and susceptibility to damage. *Arch. Ophthalmol.* 99:635
69. Quigley HA, Anderson DR. 1976. The dynamics and location of axonal transport blockade by acute intraocular pressure elevation in primate optic nerve. *Invest. Ophthalmol. Vis. Sci.* 15:606–16
70. Quigley HA, Flower RW, Addicks EM, McLeod DS. 1980. The mechanism of optic nerve damage in experimental acute intraocular pressure elevation. *Invest. Ophthalmol. Vis. Sci.* 19:505
71. Hernandez MR. 2000. The optic nerve head in glaucoma: role of astrocytes in tissue remodeling. *Prog. Retin. Eye Res.* 19:297–321
72. Yan DB, Metheetrairut A, Coloma FM, Trope GE, Heathcote JG, Ethier CR. 1994. Deformation of the lamina cribrosa by elevated intraocular pressure. *Br. J. Ophthalmol.* 78:643–48
73. Nesterov AP, Egoriv EA. 1986. Pathological physiology of primary open angle glaucoma. In *Glaucoma*, ed. J Cairns, pp. 382–96. Miami, FL: Grune Stratton
74. Yan DB, Flanagan JG, Farra T, Trope GE, Ethier CR. 1998. Study of regional deformation of the optic nerve head using scanning laser tomography. *Curr. Eye Res.* 17:903–16
75. Levy NS, Crapps EE. 1984. Displacement of optic nerve head in response to short-term intraocular pressure elevation in human eyes. *Arch. Ophthalmol.* 102:782–86
76. Levy NS, Crapps EE, Bonney RC. 1981. Displacement of the optic nerve head. Response to acute intraocular pressure elevation in primate eyes. *Arch. Ophthalmol.* 99:2166–74

77. He DQ, Ren ZQ. 1999. A biomathematical model for pressure-dependent lamina cribrosa behavior. *J. Biomech.* 32:579–84
78. Edwards ME, Good TA. 2001. Use of a mathematical model to estimate stress and strain during elevated pressure induced lamina cribrosa deformation. *Curr. Eye Res.* 23:215–25
79. Bellezza AJ, Hart RT, Burgoyne CF. 2000. The optic nerve head as a biomechanical structure: initial finite element modeling. *Invest. Ophthalmol. Vis. Sci.* 41:2991–3000
80. Sigal IA, Flanagan JG, Tertinegg I, Ethier CR. 2003. Investigation of the biomechanical environment within the optic nerve head by finite element modelling. In *Computational Fluid and Solid Mechanics 2003, Proc. Second MIT Conf.*, ed. KJ Bathe, pp. 1810–13. New York: Elsevier
81. Pau H, Kranz J. 1991. The increasing sclerosis of the lens and its relevance to accommodation and presbyopia. *Graefes Arch. Clin. Exp. Ophthalmol.* 229:294–96
82. Fisher R. 1971. The elastic constants of the human lens. *J. Physiol.* 212:147–80
83. Glasser A, Campbell M. 1998. Presbyopia and the optical changes in the human crystalline lens with age. *Vision Res.* 38:209–29
84. Koretz J, Cook C, Kaufman P. 1997. Accommodation and presbyopia in the human eye. Changes in the anterior segment and crystalline lens with focus. *Invest. Ophthalmol. Vis. Sci.* 38:569–78
85. Lütjen-Drecoll E, Tamm E, Kaufman P. 1988. Age-related loss of morphologic response to pilcarpine in rhesus monkey ciliary muscle. *Arch. Ophthalmol.* 106:1591
86. Neider M, Crawford K, Kaufman P, Bito L. 1990. In vivo videography of the rhesus monkey accommodative apparatus. Age-related loss of ciliary muscle response to central stimulation. *Arch. Ophthalmol.* 108:69
87. Fisher R. 1977. The force of contraction of human ciliary muscle during accommodation. *J. Physiol.* 270:51
88. Swegmark G. 1969. Studies with impedance cyclography on human ocular accommodation at diferent ages. *Acta Ophthalmol.* 47:1186
89. Pardue MT, Sivak JG. 2000. Age-related changes in human ciliary muscle. *Optom. Vis. Sci.* 77:204–10
90. Tamm E, Lutjen-Drecoll E, Jungkunz W, Rohen JW. 1991. Posterior attachment of ciliary muscle in young, accommodating old, presbyopic monkeys. *Invest. Ophthalmol. Vis. Sci.* 32:1678–92
91. Bill A. 1975. Blood circulation and fluid dynamics in the eye. *Physiol. Rev.* 55:383–416
92. Grunwald JE, Petrig BL, Robinson F. 1986. Retinal blood flow autoregulation in response to an acute increase in blood pressure. *Invest. Ophthalmol. Vis. Sci.* 27:1706–12
93. Wangsa-Wirawan ND, Linsenmeier RA. 2003. Retinal oxygen: fundamental and clinical aspects. *Arch. Ophthalmol.* 121:547–57
94. Parver LM, Auker C, Carpenter DO. 1980. Choroidal blood flow as a heat dissipating mechanism in the macula. *Am. J. Ophthalmol.* 89:641–46
95. Bill A. 1985. Some aspects of the ocular circulation. Friedenwald lecture. *Invest. Ophthalmol. Vis. Sci.* 26:410–24
96. Foulds W. 1990. The choroidal circulation and retinal metabolism: an overview. *Eye* 4:243–48
97. Linsenmeier RA, Padnick-Silver L. 2000. Metabolic dependence of photoreceptors on the choroid in the normal and detached retina. *Invest. Ophthalmol. Vis. Sci* 41:3117–23
98. Kiel JW, van Heuven WA. 1995. Ocular perfusion pressure and choroidal blood flow in the rabbit. *Exp. Eye Res.* 60:267–78
99. Kiel JW, Shepherd AP. 1992. Autoregulation of choroidal blood flow in the rabbit. *Invest. Ophthalmol. Vis. Sci.* 33:2399–410
100. Maepea O. 1992. Pressures in the anterior ciliary arteries, choroidal veins and

choriocapillaris. *Exp. Eye Res.* 54:731–36
101. Shapiro AH. 1977. Physiological and medical aspects of flow in collapsible tubes. *Proc. Can. Congr. Appl. Mech., 6th, Vancouver,* pp. 883–906
102. Shapiro AH. 1977. Steady flow in collapsible tubes. *J. Biomech. Eng.* 99:126–47
103. Kamm RD. 1987. Flow through collapsible tubes. In *Handbook of Bioengineering*, ed. R Skalak, S Chien. New York: McGraw-Hill
104. Cole D. 1966. Aqueous humor formation. *Doc. Ophthalmol.* 21:116–238
105. Phelps CD, Armaly MF. 1978. Measurement of episcleral venous pressure. *Am. J. Ophthalmol.* 85:35–42
106. Brubaker RF. 1967. Determination of episcleral venous pressure in the eye. A comparison of three methods. *Arch. Ophthalmol.* 77:110
107. Minckler DS, Spaeth GL. 1981. Optic nerve damage in glaucoma. *Surv. Ophthalmol.* 26:128–48
108. Brubaker RF. 1989. Measurement of aqueous flow by fluorophotometry. See Ref. 172, pp. 337–44
109. Bartels SP. 1989. Aqueous humor production. See Ref. 172, pp. 199
110. Becker B, Neufeld AH. 2002. Erratum. Pressure dependence of uveoscleral outflow. *J. Glaucoma* 11:545
111. Becker B, Neufeld AH. 2002. Pressure dependence of uveoscleral outflow. *J. Glaucoma* 11:464
112. Mäepea O, Bill A. 1989. The pressures in the episcleral veins, Schlemm's canal and the trabecular meshwork in monkeys: effects of changes in intraocular pressure. *Exp. Eye Res.* 49:645–63
113. Mäepea O, Bill A. 1992. Pressures in the juxtacanalicular tissue and Schlemm's canal in monkeys. *Exp. Eye Res.* 54:879–83
114. Ethier CR. 2002. The inner wall of Schlemm's canal. *Exp. Eye Res.* 74:161–72
115. Schottenstein EM. 1989. Intraocular pressure. See Ref. 172, pp. 301–17
116. Beck AD. 2003. Review of recent publications of the Advanced Glaucoma Intervention Study. *Curr. Opin. Ophthalmol.* 14:83–85
117. Johnson M, Kamm RD. 1983. The role of Schlemm's canal in aqueous outflow from the human eye. *Invest. Ophthalmol. Vis. Sci.* 24:320
118. Ethier CR, Kamm RD, Palaszewski BA, Johnson MC, Richardson TM. 1986. Calculation of flow resistance in the juxtacanalicular meshwork. *Invest. Ophthalmol. Vis. Sci.* 27:1741–50
119. Alexander JP, Samples JR, Acott TS. 1998. Growth factor and cytokine modulation of trabecular meshwork matrix metalloproteinase and TIMP expression. *Curr. Eye Res.* 17:276–85
120. Bradley JM, Vranka J, Colvis CM, Conger DM, Alexander JP, et al. 1998. Effect of matrix metalloproteinases activity on outflow in perfused human organ culture. *Invest. Ophthalmol. Vis. Sci.* 39:2649–58
121. Bradley JM, Kelley MJ, Zhu X, Anderssohn AM, Alexander JP, Acott TS. 2001. Effects of mechanical stretching on trabecular matrix metalloproteinases. *Invest. Ophthalmol. Vis. Sci.* 42:1505–13
122. Ethier CR. 2002. The inner wall of Schlemm's canal. *Exp. Eye Res.* 74:161–72
123. Johnson M, Erickson K. 2000. Mechanisms and routes of aqueous humor drainage. In *Principles and Practices of Ophthalmology*, ed. DM Albert, FA Jakobiec, pp. 2577–95. Philadelphia, PA: WB Saunders Co.
124. Ye W, Gong H, Sit A, Johnson M, Freddo TF. 1997. Interendothelial junctions in normal human Schlemm's canal respond to changes in pressure. *Invest. Ophthalmol. Vis. Sci.* 38:2460–68
125. Ethier CR. 2002. The inner wall of Schlemm's canal. *Exp. Eye Res.* 74:161–72
126. Deleted in proof

127. Johnson M, Shapiro A, Ethier CR, Kamm RD. 1992. The modulation of outflow resistance by the pores of the inner wall endothelium. *Invest. Ophthalmol. Vis. Sci.* 33:1670–75
128. Parc CE, Johnson DH, Brilakis HS. 2000. Giant vacuoles are found preferentially near collector channels. *Invest. Ophthalmol. Vis. Sci.* 41:2984–90
129. Grierson I, Lee WR. 1977. Light microscopic quantitation of the endothelial vacuoles in Schlemm's canal. *Am. J. Ophthalmol.* 84:234–46
130. Coleman DJ, Trokel S. 1969. Direct-recorded intraocular pressure variations in a human subject. *Arch. Ophthalmol.* 82:637–40
131. Ethier CR. 2002. The inner wall of Schlemm's canal. *Exp. Eye Res.* 74:161–72
132. Canning CR, Greaney MJ, Dewynne JN, Fitt AD. 2002. Fluid flow in the anterior chamber of a human eye. *IMA J. Math. Appl. Med. Biol.* 19:31–60
133. Heys JJ, Barocas VH. 2002. A boussinesq model of natural convection in the human eye and the formation of Krukenberg's spindle. *Ann. Biomed. Eng.* 30:392–401
134. Heys J, Barocas VH. 1999. Mechanical characterization of the bovine iris. *J. Biomech.* 32:999–1003
135. Heys JJ, Barocas VH. 2002. Computational evaluation of the role of accommodation in pigmentary glaucoma. *Invest. Ophthalmol. Vis. Sci.* 43:700–8
136. Heys JJ, Barocas VH, Taravella MJ. 2001. Modeling passive mechanical interaction between aqueous humor and iris. *J. Biomech. Eng.* 123:540–47
137. Green K, DeBarge LR, Cheeks L, Phillips CI. 1987. Centripetal movement of fluorescein dextrans in the cornea: relevance to arcus. *Acta Ophthalmol.* 65:538–44
138. Wiig H. 1990. Cornea fluid dynamics. II. Evidence for transport of radiolabelled albumin in rabbits by bulk flow. *Exp. Eye Res.* 50:261–67
139. Klyce SD. 1975. Transport of Na, Cl, and water by the rabbit corneal epithelium at resting potential. *Am. J. Physiol.* 228:1446–52
140. Mishima S, Maurice DM. 1961. The oily layer of the tear film and evaporation from the corneal surface. *Exp. Eye Res.* 1:39–45
141. Trenberth S, Mishima S. 1968. The effect of ouabain on the rabbit corneal endothelium. *Invest. Ophthalmol. Vis. Sci.* 7:44–52
142. Klyce S, Russell S. 1979. Numerical solution of coupled transport equations applied to corneal hydration dynamics. *J. Physiol.* 292:107–34
143. Kedem O, Katchalsky A. 1958. Thermodynamic analysis of the permeability of biological membranes to nonelectrolytes. *Biochim. Biophys. Acta* 27: 229–46
144. Hedbys B, Mishima S. 1962. Flow of water in the corneal stroma. *Exp. Eye Res.* 1:262–75
145. Ruberti JW, Klyce SD, Smolek MK, Karon MD. 2000. Anomalous acute inflammatory response in rabbit corneal stroma. *Invest. Ophthalmol. Vis. Sci.* 41: 2523–30
146. Overby D, Ruberti J, Gong H, Freddo TF, Johnson M. 2001. Specific hydraulic conductivity of corneal stroma as seen by quick-freeze/deep-etch. *J. Biomech. Eng.* 123:154–61
147. Fatt I, Shantinath K. 1971. Flow conductivity of retina and its role in retinal adhesion. *Exp. Eye Res.* 12:218–26
148. Marmor MF, Abdul-Rahim AS, Cohen DS. 1980. The effect of metabolic inhibitors on retinal adhesion and subretinal fluid resorption. *Invest. Ophthalmol. Vis. Sci.* 19:893–903
149. Tsuboi S. 1987. Measurement of the volume flow and hydraulic conductivity across the isolated dog retinal pigment epithelium. *Invest. Ophthalmol. Vis. Sci.* 28:1776–82
150. Marshall J, Hussain AACS, Moore DJ, Patmore AL. 1998. Aging and Bruch's membrane. In *The Retinal Pigment*

Epithelium: Function and Disease, ed. MF Marmor, TJ Wolfensberger, pp. 669–92. New York: Oxford Univ. Press
151. Negi A, Marmor MF. 1983. The resorption of subretinal fluid after diffuse damage to the retinal pigment epithelium. *Invest. Ophthalmol. Vis. Sci.* 24:1475–79
152. Bird AC, Marshall J. 1986. Retinal pigment epithelial detachments in the elderly. *Trans. Ophthalmol. Soc. UK* 105:674–82
153. Ruberti JW, Curcio CA, Millican L, Menco BPhM, Huang J-D, Johnson M. 2003. Quick-freeze/deep-etch visualization of age-related lipid accumulation in Bruch's membrane. *Invest. Ophthalmol. Vis. Sci.* 44:1753–59
154. Malek G, Guidry C, Medeiros NE, Curcio CA. 2002. Localization of apolipoproteins and cholesterol in macular and peripheral Bruch's membrane, basal deposits (BD) and drusen of normal and age-related maculopathy eyes. *Invest. Ophthalmol. Vis. Sci.* 43:2789 (Abstr.) www.arvo.org
155. Curcio CA, Millican CL, Bailey T, Kruth HS. 2001. Accumulation of cholesterol with age in human Bruch's membrane. *Invest. Ophthalmol. Vis. Sci.* 42:265–74
156. Moore DJ, Clover GM. 2001. The effect of age on the macromolecular permeability of human Bruch's membrane. *Invest. Ophthalmol. Vis. Sci.* 42:2970–75
157. Ambati J, Gragoudas ES, Miller JW, You TT, Miyamoto K, et al. 2000. Transscleral delivery of bioactive protein to the choroid and retina. *Invest. Ophthalmol. Vis. Sci.* 41:1186–91
158. Geroski DH, Edelhauser HF. 2001. Transscleral drug delivery for posterior segment disease. *Adv. Drug Deliv. Rev.* 52:37–48
159. Hamalainen KM, Kananen K, Auriola S, Kontturi K, Urtti A. 1997. Characterization of paracellular and aqueous penetration routes in cornea, conjunctiva, and sclera. *Invest. Ophthalmol. Vis. Sci.* 38:627–34
160. Ambati J, Canakis CS, Miller JW, Gragoudas ES, Edwards A, et al. 2000. Diffusion of high molecular weight compounds through sclera. *Invest. Ophthalmol. Vis. Sci.* 41:1181–85
161. Boubriak OA, Urban JP, Bron AJ. 2003. Differential effects of aging on transport properties of anterior and posterior human sclera. *Exp. Eye Res.* 76:701–13
162. Levick JR. 1987. Flow through interstitium and other fibrous matrices. *Q. J. Exp. Physiol.* 72:409–37
163. Fatt I, Hedbys BO. 1970. Flow of water in the sclera. *Exp. Eye Res.* 10:243
164. Bill A. 1964. The drainage of albumin from the uvea. *Exp. Eye Res.* 3:179
165. Pederson JE, Gaasterland DE, MacLellan HM. 1977. Uveoscleral aqueous outflow in the rhesus monkey: importance of uveal reabsorption. *Invest. Ophthalmol. Vis. Sci.* 16:1008
166. Bill A, Phillips CI. 1971. Uveoscleral drainage of aqueous humor in human eyes. *Exp. Eye Res.* 12:275–81
167. Crawford K, Kaufman PL. 1987. Pilocarpine antagonizes prostaglandin F2 alpha-induced ocular hypotension in monkeys. Evidence for enhancement of Uveoscleral outflow by prostaglandin F2 alpha. *Arch. Ophthamol.* 105:1112–16
168. Lütjen-Drecoll E, Tamm E. 1988. Morphological study of the anterior segment of cynomolgus monkey eyes following treatment with prostaglandin $F_{2\alpha}$. *Exp. Eye Res.* 47:761–69
169. Gabelt B, Kaufman P. 1989. Prostaglandin F increases uveoscleral outflow in the cynomolgus monkey. *Exp. Eye Res.* 49: 389–402
170. Bill A. 1966. Conventional and uveoscleral drainage of aqueous humor in the cynomologous monkey (macaca irus) at normal and high intraocular pressures. *Exp. Eye Res.* 5:45
171. Ruberti JW, Klyce SD. 2003. NaCl osmotic perturbation can modulate hydration control in rabbit cornea. *Exp. Eye Res.* 76:349–59
172. Ritch R, Shields MB, Krupin T, eds. 1989. *The Glaucomas*. St. Louis, MO: C.V. Mosbey Co.

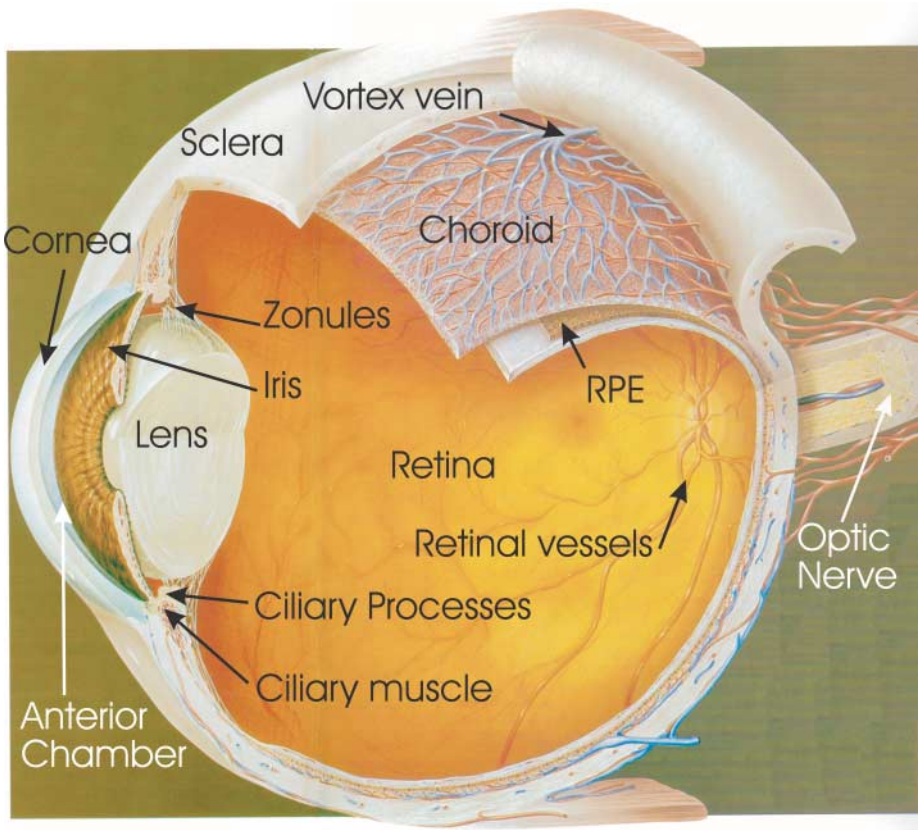

Figure 1 Overview of ocular anatomy, with several key ocular components labelled. Modified from (2).

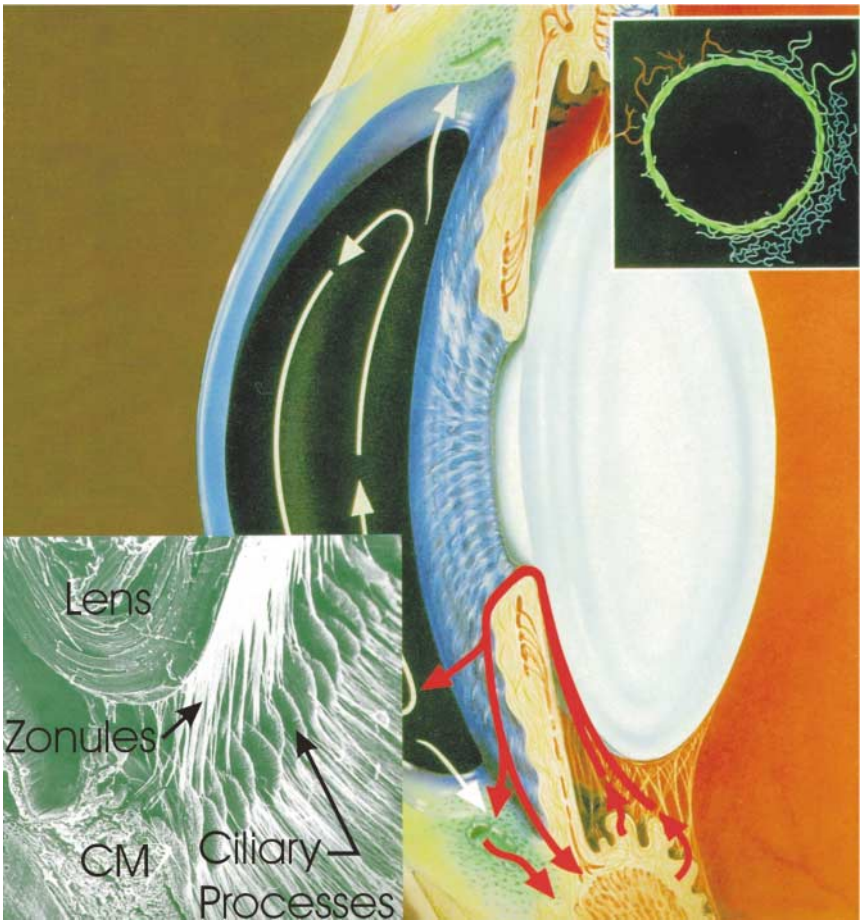

Figure 4 View of anterior segment of eye, showing site of production of aqueous humor (ciliary processes) and drainage routes (*red arrows*). The white arrows in the anterior chamber show thermal convection patterns. The lower left inset is a scanning electron micrograph of the zonular apparatus (CM = ciliary muscle). The inset at upper right shows Schlemm's canal (*green*) as seen face-on. Green vessels anatomising with Schlemm's canal are collector channels; blue vessels are aqueous veins; red vessels are arterioles. Modified from (2).